Int. J. Electrochem. Sci., 10 (**2015**) 4888 - 4898

International Journal of
ELECTROCHEMICAL
SCIENCE
www.electrochemsci.org

Electrochemical Behavior of Zirconium in Succinic Acid Solution

Gamal A. EL-Mahdy[1,2,*], *Mohammed Abdel-Reheem*[3,4] , *Samir A. Abdel-Latif* [2], *A. A F. Zikry*[2]

[1]Department of Chemistry, College of Science, King Saud University, Riyadh 11451, Kingdom of Saudi Arabia
[2]Chemistry department, Faculty of Science, Helwan University,Ain- Helwan, 11795, Cairo, Egypt.
[3]Research Center, College of Science, King Saud University, Riyadh, Saudi Arabia
[4]Biochemistry Department, Faculty of Agriculture, Ain Shams University, Cairo, Egypt
[*]E-mail: gamalmah2000@yahoo.com

Received: 17 November 2014 / *Accepted:* 28 March 2015 / *Published:* 28 April 2015

The influence of succinic acid concentrations on the electrochemical behavior of ZrO_2 has been investigated using open circuit potential (OCP), electrochemical impedance spectroscopy (EIS) and galvanostatic techniques. The anodic oxidation of zirconium leads to a significant improvement in the corrosion resistance of zirconium in succinic acid solution. OCP gradually increases towards noble values in 0.01 M succinic acid, while it decreases slowly to less noble values in 0.1 M succinic acid during the initial stage of monitoring and eventually attains a steady state. The film stability dependent upon the succinic acid concentration as evident from a shift in OCP values to less noble values with increasing concentration. The results of polarization indicates that the passive layers increase in thickness with decreasing acid concentration and become less susceptible to corrosion and thus providing more protection of the underlying zirconium metal.

Keywords: Zirconium, polarization, OCP, EIS, Galvanostatic, succinic acid

1. INTRODUCTION

Zirconium has excellent corrosion resistance in different acids and alkalis solutions. The excellent corrosion resistance of zirconium can be attributed to the crystal structure and stability of ZrO_2 film formed. Nanotube zirconia and nanoporous and has great potential applications in the fields of adsorption , heterogeneous catalysis , chemical sensors , separation , electronics, optics, biomedical implants, and magnetics [1–4]. Preparation of ZrO2 nanotubes by anodization, and the effect of electrochemical parameters such as applied potential [6], sweep rate [7], electrolytic composition [5], and anodization time [8] on the formation of ZrO_2 nanotubes has been investigated. It has been widely

applied as sensors [9], catalyst support [10], and in biomedical implants [11–13]. The low neutron absorption coefficient is the main reason for application of zirconium in the nuclear industry. Zirconium and its alloys have been studied extensively [14–18]. The mechanical properties of zirconium along with the electrochemical resistance of zirconium are the main reason for application in thermal nuclear reactors of separating the coolant water from the nuclear fuel [19]. The superior mechanical properties , high dielectric constant , chemical stability, electrical and wide band gap of ZrO_2 are the main reasons for applications in electronics, magneto-electronics, optics, and optoelectronics Recently, ZrO_2 nanoporous or nanotubular structures have been achieved via anodization in fluoride containing electrolytes [32–33]. ZrO_2 has high density of 5.83 g/cm3, high melting point of 2400 oC, a high fracture toughness of 17.2 MPa.m0.5, chemical inertness, and a micro hardness of 700 (Vickers scale) [34], which considered as the key material properties of ZrO_2. This property makes it a special contender for optical applications. For several decades, ZrO_2 was found in applications such as refractory materials, ceramics, hard coatings etc. Recently, ZrO_2 was scrutinized for application in the electronic industry as promising candidate for replacing SiO_2 as gate oxide, because of its electronic properties. In addition, it has the excellent ability to respond or filter some specific portions of the electromagnetic spectrum. It was reported that the ZrO2 thin films can be deposited using several techniques, such as pulsed laser deposition (PLD) chemical vapor deposition (CVD), physical vapor deposition (including sputtering and e-beam deposition) and atomic layer deposition (ALD), and [35-37]. Kulki et al. [38] deposited ZrO2 films by exploiting several organo-metallic precursors in metal oraganic chemical vapor deposition (MOCVD) method, at substrate temperatures ranging from 180 to 600 oC. Cassir and his co-researchers [39] reported that the deposition temperature affects crystal structure, growth kinetics (i.e., film thickness), and surface morphology. Chatterji et al. [40] demonstrated plasma enhanced CVD deposition of ultra thin ZrO2 films with effective oxide thickness 28 A and electrically characterized the films. Sawa et al. [41] deposited ZrO2 thin films using radio frequency reactive sputter deposition with varying Ar/O2 partial pressure ratio. The effect of Zr/Si molar ratio on morphology, structure and protection performance of organosilane coatings doped with zirconium(IV) n-propoxide has been investigated . The results indicated that the addition of zirconium(IV) n-propoxide promoted the formation of silica network and enhanced the compactness of coating matrix [42] . The evaluation of a zirconium dioxide composite membrane on the performance of a methanol fuel cell has been investigated [43]. The results revealed that the composite zirconium membrane had better performance than that obtained from the commercial membrane. Herein, the results of electrochemical behavior of zirconium in succinic acid solution are reported. The anodization of zirconium was carried out in aqueous solutions of succinic acid with different concentrations and the corrosion resistance of zirconium was evaluated using an open circuit, polarization measurements and EIS techniques.

2. EXPERIMENTAL RESULTS

2.1. Specimen preparation

Pure zirconium rod (Johnson- Matthey, London) was used for preparation of zirconium electrode , which connected to copper wire using silver paste and the connection was secured using

quick dry epoxy. The sample was fixed in epoxy resin and served as working electrode. Specimens were ultrasonically cleaned using deionized (DI) water, acetone, and ethanol sequentially and finally dried using compressed air before each experiment,. Samples were then treated by dip etching in a solution containing $HF/HNO_3/H_2O$ (volume ratio, 1:4:2) for 1 second [44-45].

2.2 Electrochemical measurements

Electrochemical investigations were carried out in succinic acid solution using three-electrode electrochemical cell consisting of Pt as a counter electrode, Zr as working electrode , and SCE as a reference electrode. All electrochemical measurements were carried out with a SI 1287 Solartron (potentiostat/galvanostat) and Solartron 1260 as frequency response analyzer. The potentiodynamic polarization curves were conducted using a scan rate of 1 mV s^{-1} and electrochemical impedance spectra were performed in the 10^4–10^{-2} Hz frequency range.The software packages; Corr Ware, Corr View and Zview provided by Solartron were used to measure and analyze the data.

3. RESULTS AND DISCUSSION

3.1 Open circuit potential measurements

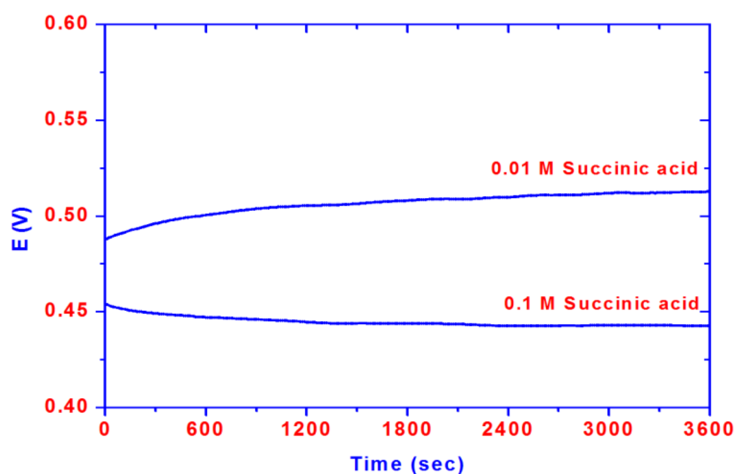

Figure 1. Evolution of OCP with time at different succinic acid concentrations.

Monitoring data of open circuit potential (OCP) at different succinic acid concentrations is shown in Fig. 1. It is evident that OCP gradually increases towards a noble values as time progresses and eventually reaches a steady state in 0.01 M succinic acid. OCP decreases slowly to less noble values with time and finally attains a steady state in case of 0.1 M succinic acid. The results can be explained on the bases of natural formation of thick oxide film of barrier type passive film [46] in 0.01 M succinic acid, which leads to a shift in potential to more noble values. The decay of OCP with time

observed in 0.1 M succinic acid can be attributed to the defective character and heterogeneity of the passive film formed. It provides assessable sites for the rupture of the passive film leading to its breakdown. The shift in potential to less noble values can be attributed to cumulative effect of the defective passive character, which leads to an unstable passive film with more susceptibility to dissolution.

It is known that a natural developed oxide film is formed successively with time in H_2SO_4 [47] and HNO_3 [48] depending upon acid concentration. ZrO_2 dissolved in succinic acid solution as [49-51]:

$$ZrO_2 + 4H^+ + 4e^- \rightarrow 2H_2O + Zr \quad (1)$$

3.2. Potentiodynamic polarization results

Potentiodynamic polarization study in 0.01-0.1 M succinic acid is shown in Fig. 2. The polarization curve did not display any active-passive transition behavior. The polarization curve displays a pronounced effect on the anodic polarization with increasing succinic acid concentration. Polarization parameters were calculated and quoted in Table 1. It is clear that corrosion rate was doubled and Ecorr was sifhted to less noble values with increasing succinic acid concentration. Polarization curve in 0.01 M succinic acid displayed a wider passive rage than that experienced in higher concentration. It is established that the homogeneity of the formed passive film is strongly affecting the passive current density. The dissolution and the changes in the nature of passive film increase with an increase in the concentration of succinic acid solution. The results show that, as the passive layers increase in thickness with decreasing the acid concentration, they become less susceptible to corrosion and thus increasingly provide more protection of the underlying zirconium metal.

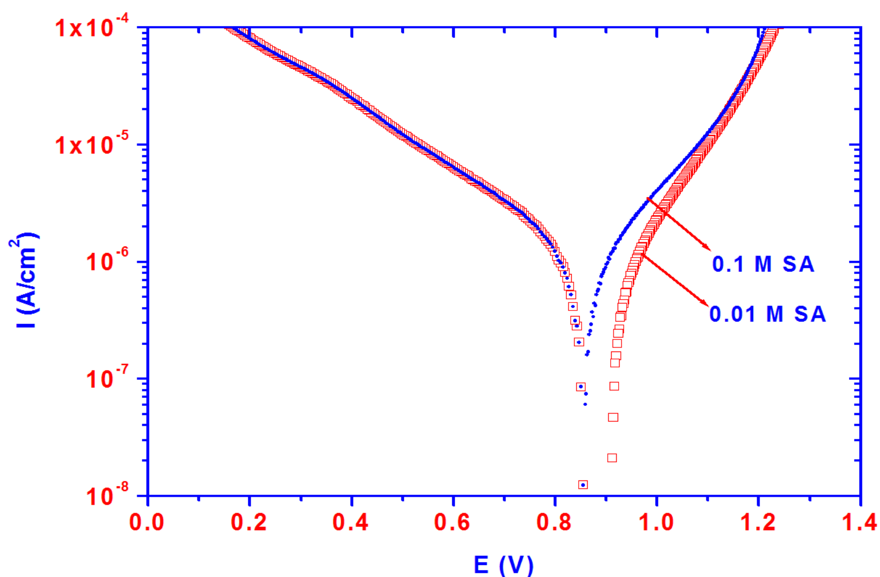

Figure 2. Potentiodynaimcs polarization of zirconium in different succinic acid concentrations.

Table 1. Polarization parameters of zirconium in 0.01 and 0.1 M succinic acid solution.

Acid conc. (M)	Icorr ($\mu A/cm^2$)	Ecorr (V)
0.01	0.55	0.9124
0.1	1.02	0.8563

A less negative corrosion potential value experienced in 0.01 M succinic acid reveals a more stable passive layer (more noble), as well as further protection of the zirconium to corrosion in succinic solution. The higher values of the recorded potential experienced in lower succinic acid concentration can be explained on the basis of formation of thicker outer layers over thinner barrier ones, which is consistent with the previously reported data for the formation of the passive film formed on zirconium in phosphoric acid solution [52]. Both cathodic and anodic polarization curves were significantly shifted to lower current densities in low concentrated succinic acid solution as compared to the higher one. Moreover, the corrosion potentials of exhibited in low concentrated solution showed a considerable shift in the noble direction.

3.3 Anodization of zirconium

Galvanostatic anodization of zirconium in succinic acid with different concentrations (0.01-0.1 M) using 5 mA/cm^2 is shown in Fig. 3. It can be seen that the voltage rises linearly and reaches maximum during the initial stage of anodization as shown in the inserted Fig.3. The voltage drops to a low value then attains a steady state during the last stage of anodization. The energy resulted from the oxide film growth cause a fracture of the oxide film during the observed breakdown occurred in the initial stage of the anodization. The restriction of the oxide film growth increases with increasing succinic acid concentration. It is evident that an increase in succinic concentrations causes a decrease in the maximum and the steady state attaining potential.

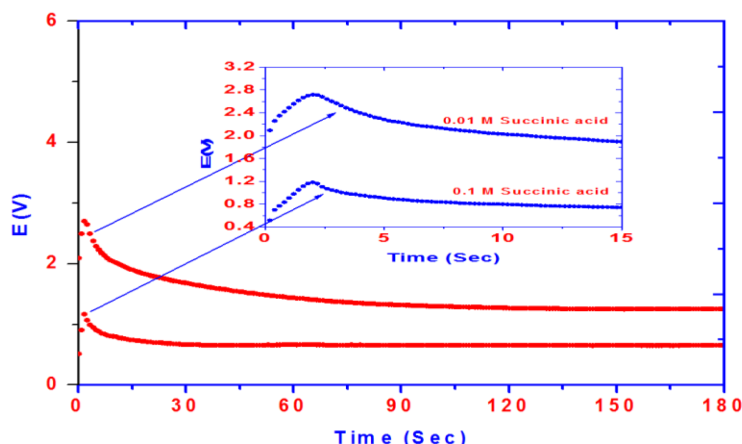

Figure 3. Variations of potential with time during anodization of zirconium at different succinic acid concentrations.

Two processes occurred during the oxide film growth. The first process is the oxide film growth and the second is the oxide film dissolution. The former process is the predominant during the initial stage of oxide film growth. The latter process is the predominant process during dropping the voltage to lower value. The equal processes of the oxide film growth and dissolution leads to a steady state observed during the last stage of anodization. The positive shift in the potential experienced during the initial stage of the anodic polarization can be accounted to the adsorption of hydroxyl ions. As the potential continuously shifted in the noble direction, the oxide film formed withstands further dissolution of zirconium from the surface and becomes a predominant process. As consequence, the potential shifts to less noble values during the end of the initial stage of anodization. The ionic current passed through the barrier oxide film during the anodization of zirconium in succinic acid solution is considered as the major part of the passed total current and increases in the oxide film thickness. The succinic acid solution in contact with zirconium, injects electrons into the conduction band of the anodic oxide. This process are enhanced by the anodization field, which stimulates avalanches by an impact ionization mechanism [53].The voltage breakdown occurs when the avalanche electronic current reaches critical value and cannot grow exponentially as anodizing time increases during the initial stage of anodization as shown in Fig 3 (inset). This stage is characterized by the deflection in potential–time curve and followed by a continuous decrease in voltage as time progresses. During the initial stage before voltage breakdown, the potential increases sharply to a maxima due to a continuous growth of a compact barrier oxide film. After the breakdown, voltage decreases with time, which may be attributed to a continuous decrease in the thickness of the formed oxide film.

3.4. Electrochemical impedance spectroscopy

The impedance behavior for zirconium metal at different immersion times was measured in the frequency range of 10 kHz to 0.01 Hz and the Bode plots after 30 and 120 minutes immersion are shown in Figs. 4 and 5 respectively. Nyquist plots at different immersion times are shown in Figure 6.

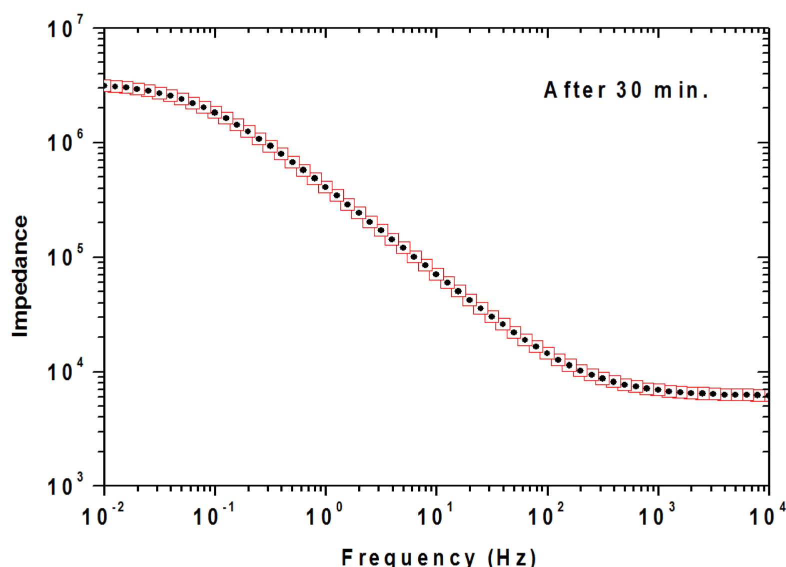

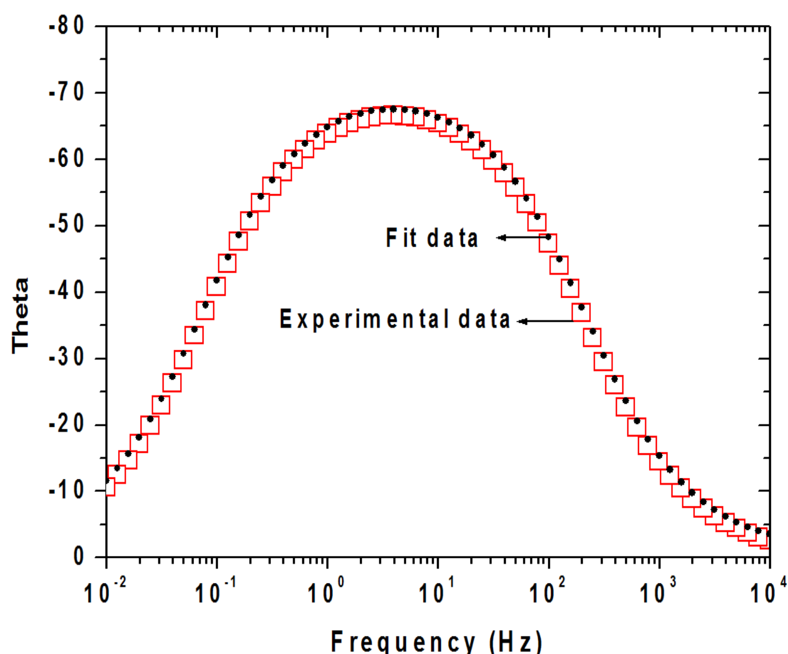

Figure 4. Bode impedance plots for zirconium after 30 minutes immersion in 0.01M succinic acid concentration showing the experimental and fitted data.

The best possible fit equivalent circuit model is shown in Fig. 7 The equivalent circuit model shown in Fig. 7 , consists of a solution resistance Rs in series to the constant phase element CPE and the charge transfer resistance Rct. The use of a CPE is required for modeling the frequency dispersion generally related to the surface heterogeneity due to impurities or dislocations [54], distribution of activity centers, surface roughness, fractal structures, and formation of porous layers [55–58]. The equivalent circuit employed to describe the oxide film / solution interface is reasonably related to the corrosion process of zirconium in succinic acid solution. The impedance of CPE was used to replace double layer capacitance (Cdl) for a more accurate fit, which is described as follows [59–61]:

$$Z_{CPE} = Y_0^{-1} (J\omega)^{-n} \quad (2)$$

where Y_0 is a proportional factor, $j^2 = -1$ is an imaginary number, and ω is the angular frequency ($\omega = 2\pi f$) . If n = 1, the impedance of CPE is identical to that of a capacitor a ($Z_{CPE} = C$, n = 1), and in this case Y_0 gives a pure capacitance (C). Depending on the value of n, CPE can represent a Warburg impedance ($Z_{CPE} = W$, n = 0.5), a resistance ($Z_{CPE} = R$, n = 0), and inductance ($Z_{CPE} = L$, n = -1). In all cases, the employed CPE used to fit the experimental impedances data is associated with capacitive behavior of zirconium.

Gauge of the heterogeneity or roughness of the surface [62]. The calculated capacitance is used to estimate the film thickness, L as:

$$L = \varepsilon\varepsilon_o / X \quad (3)$$

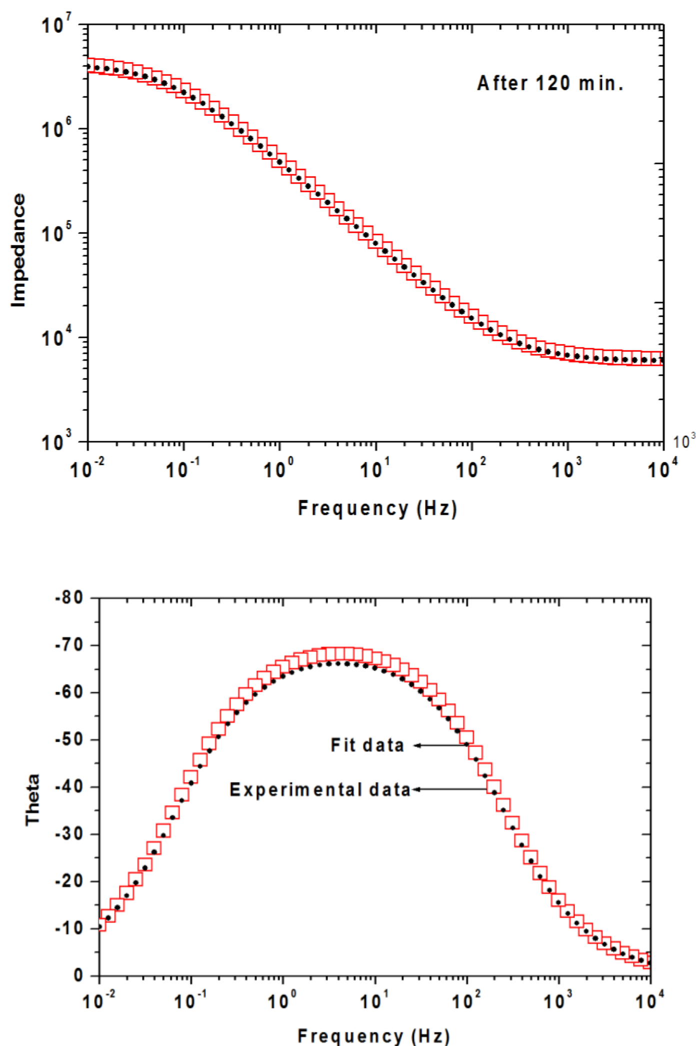

Figure 5. Bode impedance plots for zirconium after 120 minutes immersion in 0.01M succinic acid concentration showing the experimental and fitted data.

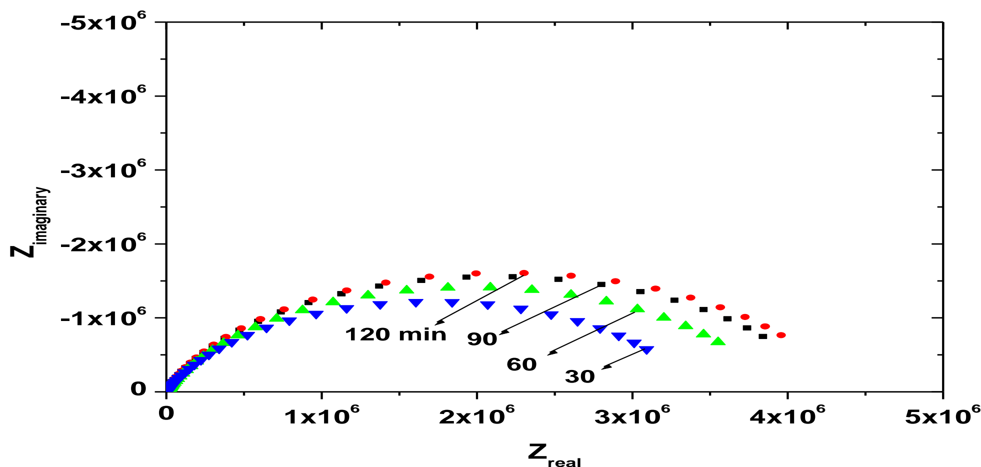

Figure 6. Nyquist impedance plots for zirconium at different immersion times in 0.01M succinic acid concentration

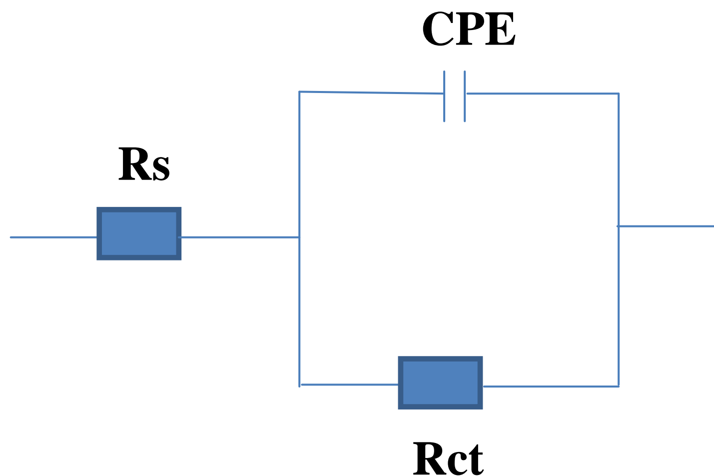

Figure 7. Equivalent circuit used for fitting the impedance data in 1 M HCl solution.

where ε_o is the vacuum permittivity (8.85 · 10^{-}14 F/ cm) and $\varepsilon = 22$ [63] is the dielectric constant of the passive film (ZrO_2). It is assumed that the passive film formed in the succinic acid solution had the same value. The measured capacitance is used to calculate the film thickness of zirconium, which is a linear relation with immersion time as shown in Fig. 8. The longer the immersion time, the thicker the formed oxide film.

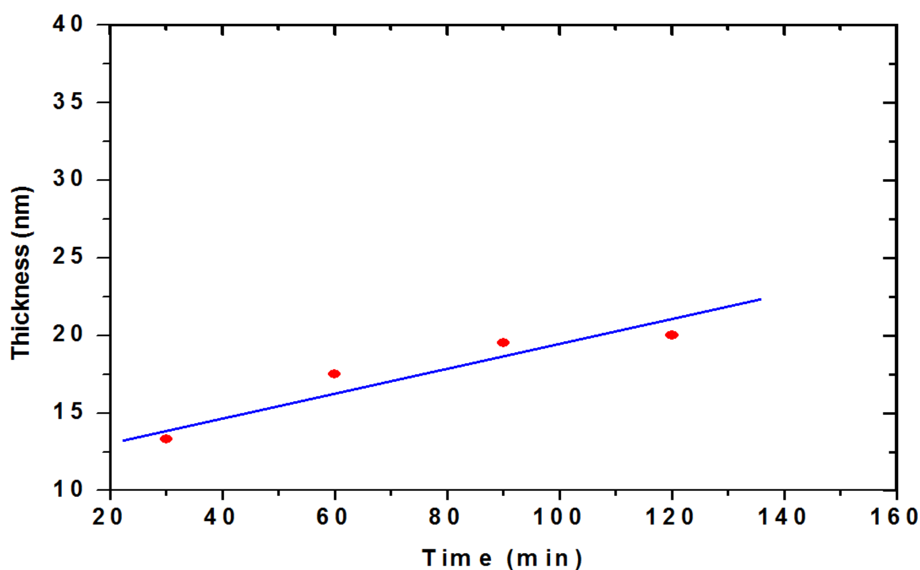

Figure 8. Dependence of zirconium film thickness on immersion time

4. CONCLUSIONS

1- The increase in succinic acid concentration resulted in the excessive dissolution of ZrO_2.

2- Open circuit potential gradually increases towards noble values with decreasing the acid concentration as time progresses and eventually attains a steady state value.

3- The passive layers increase in thickness with decreasing acid concentration and become less susceptible to corrosion providing more protection of the underlying zirconium metal.

4- The restriction of the oxide film growth increases with increasing succinic acid concentration.

ACKNOWLEDGEMENT
This project was supported by King Saud University, Deanship of Scientific Research, College of Science Research Center.

References

1. J. Bao, C. Tie, Z. Xu, Q. Ma, J. Hong, H. Sang, D. Sheng, *Adv. Mater*. 14 (2002) 44.
2. D.F. Gu, H. Baumgart, N. Gon, T. Abdel-Fattah, *Electrochem. Solid State Lett*. 12 (2009) K25.
3. H. Shin, D.K. Jeong, J. Lee, M.M. Sung, J. Kim, *Adv. Mater*. 16 (2004) 1197.
4. M.C. Tsai, G.T. Lin, H.T. Chiu, C.Y. Lee, *J. Nanopart. Res*. 10 (2008) 863.
5. H. Tsuchiya, J.M. Macak, L. Taveira, P. Schmuki, *Chem. Phys. Lett*. 410 (2005) 188.
6. H. Tsuchiya, P. Schmuki, *Electrochem. Commun*. 6 (2004) 1131.
7. H. Tsuchiya, J.M.Macak, A.Ghicov, L. Taveira, P. Schmuki, *Corros. Sci*. 47 (2005) 3324.
8. H. Tsuchiya, J.M. Macak, I. Sieber, P. Schmuki, *Small* 1 (2005) 722.
9. I. Noriya, S. Woosuck, M. Ichiro, M. Norimitsu, N. Oh-hori, I. Masaki, Sens.*Actuators, B, Chem*. 108 (2005) 216.
10. S.N. Lvov, X.Y. Zhou, G.C. Ulmer, H.L. Barnes, D.D. Macdonald, S.M. Ulyanov, L.G. Benning, D.E. Grandstaff, M. Manna, E. Vicenzi, *Chem. Geol*. 198 (2003) 141.
11. J. Chevalier*, Biomaterials* 27 (2006) 535.
12. W. Lee, W.H. Smyrl, *Curr. Appl. Phys*. 8 (2008) 818.
13. J. Zhao, X. Wang, R. Xu, F. Meng, L. Guo, Y. Li, *Mater. Lett*. 62 (2008) 4428.
14. ICONE10, Proceedings of the 10th International Conference on Nuclear Engineering, American Society of Mechanical Engineers, New York, 2002.
15. ICONE12, Proceedings of the 12th International Conference on Nuclear Engineering, American Society of Mechanical Engineers, New York, 2004.
16. A. M. Garde., E. R. Bradley (Eds), Zirconium in the Nuclear Industry: Tenth International Symposium, ASTM Special Technical Publication, Vol. 1245, Philadelphia, PA, 1994.
17. A. Goossens, M. Vazquez , D. D. Macdonald , *Electrochim. Acta* 41(1996) 47.
18. 18. G. D. Moan, P. Rudling (Eds.), *Zirconium in the Nuclear Industry: Thirteenth International Symposium,* ASTM, West Conshohocken, PA, 2002.
19. D. Zander, U. Kuster , *Mate. Sci. Eng*. A 375-377 (2004) 53.
20. H. Tsuchiya, V.Macak , I. Sieber , P. Schmuki, *Small* 1 (2005)722.
21. H. Tsuchiya, P. Schmuki , *Electrochem. Comm.* 6 (2004)1131.
22. W. J. Lee, W. H. Smyrl , *Electrochem. Solid Sate* 8 (2005) B7.
23. H. Tsuchiya , J. M. Macak, L. Taveira , P. Schmuki . *Chem. Phys. Lett.* 410 (2005)188.
24. 24. H. Tsuchiya, J. M Macak , I. Sieber I. , Schmuki P. *Material Science Forum* 512 (2006) 205.
25. W. J. Lee, W. H. Smyrl, *Curr. Appl. Phys.* 4 (2005) 36.
26. H. Tsuchiya , J. M. Macak, A. Ghicov , L. Taveira , P. Schmuki . *Corros. Sci.* 47 (2005) 324 .

27. I. Noriya , S. Woosuck , M. Ichiro M. Norimitsu, N. Oh-hori, I. Masaki , *Sens. Act., Bull. Chem.* 108 (2005) 216,.
28. S. N. Lvov ,X. Y. Zhou , G. C. Ulmer, H. L. Barnes , D. D. Macdonald , S. M. Ulyanov, L.G. Benning , Grandstaff D.E.,. Manna M, Vicenzi E., *Chem. Geol.* 198 (2003) 141.
29. Chevalier J., *Biomaterials* 27(2006) 535.
30. W. Lee ,W. H. Smyrl , *Curr. Appl . Phys.* 8 (2008) 818 .
31. J. Zhao, X. Wang , R. Xu, F. Meng ,L. Guo, Y. Li , *Mat. . Let.*10 (2008) 4428.
32. S. Berger, F. Jakubka , P. Schmuki , *Electrochem. Comm* 10 (2008)1916.
33. R. Hahn, S. Berge, P. Schmuki , *J, Solid State Electrochem.* 14 (2010) 285.
34. R. S Lima, A Kucuk and C.C. Berndt, *Surface coatings and technology* 135 (2001)166 .
35. J. Robertson, *Journal of Vacuum Science and Technology*. 18 (2000) 1785.
36. G. D. Wilk, R.M. Wallace, J.M Anthony, *Journal of Applied Physics*, 89 (2001) 5243
37. J.P.Maria *Journal of Applied Physics* 90 (2001) 448.
38. K. Kukli, M. Ritala, J. Aari, T. Uustare and M. leskela, *Journal of.Applied Physics* 92 (2002) 1833.
39. M. Cassir, F. Goubin, C. B., P. Vernoux and D. lincot, *Applied Surface Science* 193 (2002) 120.
40. S. Chatterjee, S.K. Samanta, H.D. Banerjee and C.K. Maiti, *Bulletin of Materials*
41. *Science*, 24 (2001) 579.
42. 41. Akira Sawa, Kazuki Nakanishi and Teiichi Hanada, *Thin solid films* 516 (2008) 4665.
43. 42- C. Fu, Z. W. Zhan, M.Yu , S.M. Li, J. H. Liu, L. Dong, *Int. J. Electrochem. Sci.*, 9 (2014) 2603.
    43- C. Guzmán, A. Alvarez , Luis A. Godínez , J. Ledesma–García1, L. G. Arriaga, *Int. J. Electrochem. Sci.*, 7 (2012) 6106.
44. S. Berger, J. Faltenbacher, S. Bauer, P. Schmuki, *Phys. State Solid RRL* 2(2008) 102.
45. P. Walker . W. H. Tarn (ed.) CRC Handbook of Meal Etchants, CRC Press, Boca Raton, 2000, pp. 1360.
46. A. Gebert , U. Kuehn , S. Baunack , N. Mattern, L. Schultz , *Mater. . Sci. Eng. A* vol. 415 p.242, 2006.
47. G. A. EL-Mahdy , S. S. Mahmoud , H. A. EL-Dahanm, *Thin Solid Films* 285(1996) 289.
48. N. Padhy , S. Ningshen , U. Kamachi M. Mudalim , *J Alloy, Comp,* 503 (2010) 50.
49. M. Pourbaix , Atlas of Electrochemical Equilibria in Aqueous Solutions, Nace, Houston, 1974.
50. D. J. Blackwood , L. M. Peter , D.E . Williams., *Electrochim, Acta* 33 (1988) 1143.
51. F. Bentiss, M. Lagrenee, M. Traisnel, J.C. Hornez, *Corros. Sci*. 41 (1999) 789.
52. A. Goossens, M. Vazquez, D. D. Macdonald, *Electrochim. Acta* 41 (1996) 35.
53. J. M. Albella, I. Montero, J. M. Martinez-Duart, *Electrochim. Acta* 32 (1987) 255.
54. R. Solmaz, *Corros. Sci*. 79 (2014) 169.
55. F. Zhang, Y. Tang, Z. Cao, W. Jing, Z. Wu, Y. Chen, *Corros. Sci*. 61 (2012) 1.
56. 56. W.H. Mulder, J.H. Sluyters, *Electrochim. Acta* 33 (1988) 303.
57. F.B. Growcock, V.R. Lopp, *Corros. Sci*. 28 (1988) 397.
58. M. Lagren, B. Mernari, N. Chaibi, M. Traisnel, H. Vezin, F. Bentiss *Corros. Sci*. 43 (2001) 951.
59. H. Ashassi-Sorkhabi, B. Shaabani, D. Seifzadeh, *Electrochim. Acta* 50 (2005) 3446.
60. M. Tourabi, K. Nohair, M. Traisnel, C. Jama, F. Bentiss, *Corros. Sci*. 75 (2013) 123.
61. B. Xu, Y. Liu, X. Yin, W. Yang, Y. Chen *Corros. Sci*. 74 (2013) 206.
62. D. A. Lopez, S. N. Simison , S. R. de. Sanchez , *Electrochim. Acta* 48 (2003) 845.
63. B. Cox, F. Gascoin,Y. M. Wong , *J. Nucl. Mater.*vol. 113 (1995)113.

© 2015 The Authors. Published by ESG (www.electrochemsci.org). This article is an open access article distributed under the terms and conditions of the Creative Commons Attribution license (http://creativecommons.org/licenses/by/4.0/).